

# CHEMISTRY

## A European Journal

A Journal of



### Accepted Article

**Title:** An enzymatic route to  $\alpha$ -tocopherol synthons: Aromatic hydroxylation of pseudocumene and mesitylene with P450 BM3

**Authors:** Alexander Dennig, Alexandra Maria Weingartner, Tsvetan Kardashliev, Christina Andrea Müller, Erika Tassano, Martin Schürmann, Anna Joëlle Ruff, and Ulrich Schwaneberg

This manuscript has been accepted after peer review and appears as an Accepted Article online prior to editing, proofing, and formal publication of the final Version of Record (VoR). This work is currently citable by using the Digital Object Identifier (DOI) given below. The VoR will be published online in Early View as soon as possible and may be different to this Accepted Article as a result of editing. Readers should obtain the VoR from the journal website shown below when it is published to ensure accuracy of information. The authors are responsible for the content of this Accepted Article.

**To be cited as:** *Chem. Eur. J.* 10.1002/chem.201703647

**Link to VoR:** <http://dx.doi.org/10.1002/chem.201703647>

Supported by  
**ACES**

WILEY-VCH

**Submission to: Chemistry – A European Journal**

Manuscript type: Full Paper

# An enzymatic route to $\alpha$ -tocopherol synthons: Aromatic hydroxylation of pseudocumene and mesitylene with P450 BM3

*Alexander Dennig<sup>[a]‡\*</sup>, Alexandra Maria Weingartner<sup>[a]‡</sup>, Tsvetan Kardashliev<sup>[a]</sup>, Christina Andrea Müller<sup>[a]†</sup>, Erika Tassano<sup>[c]</sup>, Martin Schürmann<sup>[d]</sup>, Anna Joëlle Ruff<sup>[a]\*</sup> and Ulrich Schwaneberg<sup>[a,b]\*</sup>*

[a] RWTH Aachen University, Institute of Biotechnology, Worringerweg 3, 52074 Aachen, Germany

[b] DWI –Leibniz Institut für Interaktive Materialien, Forckenbeckstraße 50, 52074 Aachen, Germany

[c] Department of Chemistry, University of Graz, Heinrichstrasse 28, 8010 Graz, Austria

[d] DSM Ahead R&D BV | DSM Innovative Synthesis, Post address: P.O. Box 1066, 6160 BB Geleen, The Netherlands

‡ Alexander Dennig and Alexandra M. Weingartner are joint first authors.

\*Corresponding authors: alexander.dennig@tugraz.at, aj.ruff@biotec.rwth-aachen.de  
u.schwaneberg@biotec.rwth-aachen.de

**Supporting information for this article is available on the WWW under  
<http://dx.doi.org/10.1002/chem.2017xxxx>**

## Abstract

The aromatic hydroxylation of pseudocumene (**1a**) and mesitylene (**1b**) with P450 BM3 yields key phenolic building blocks for  $\alpha$ -tocopherol synthesis. The P450 BM3 wild-type (WT) catalyzed selective aromatic hydroxylation of **1b** (94%), whereas **1a** was hydroxylated to a large extent on benzylic positions (46-64%). Site-saturation mutagenesis generated a new P450 BM3 mutant, herein named “variant M3” (R47S, Y51W, A330F, I401M), with significantly increased coupling efficiency (3 to 8-fold) and activity (75 to 230-fold) for **1a** and **1b** conversion. Additional  $\pi$ - $\pi$  interactions introduced by mutation A330F improved not only productivity and coupling efficiency, but also selectivity toward aromatic hydroxylation of **1a** (61 to 75%). Under continuous NADPH-recycling the novel P450 BM3 variant M3 was able to produce the key tocopherol precursor trimethylhydroquinone (TMHQ, **3a**) (35% selectivity; 0.18 mg ml<sup>-1</sup>) directly from **1a**. In case of **1b** over-oxidation leads to dearomatization and formation of a valuable *p*-quinol synthon that can directly serve as educt for synthesis of **3a**. Detailed product pattern analysis, substrate docking and mechanistic considerations support the hypothesis that **1a** binds in an inverted orientation in the active site of P450 BM3 WT as compared to P450 BM3 variant M3 to allow this change in chemo-selectivity. This study provides an enzymatic route to key phenolic synthons for  $\alpha$ -tocopherols and the first catalytic and mechanistic insights into direct aromatic hydroxylation and dearomatization of trimethylbenzenes with O<sub>2</sub>.

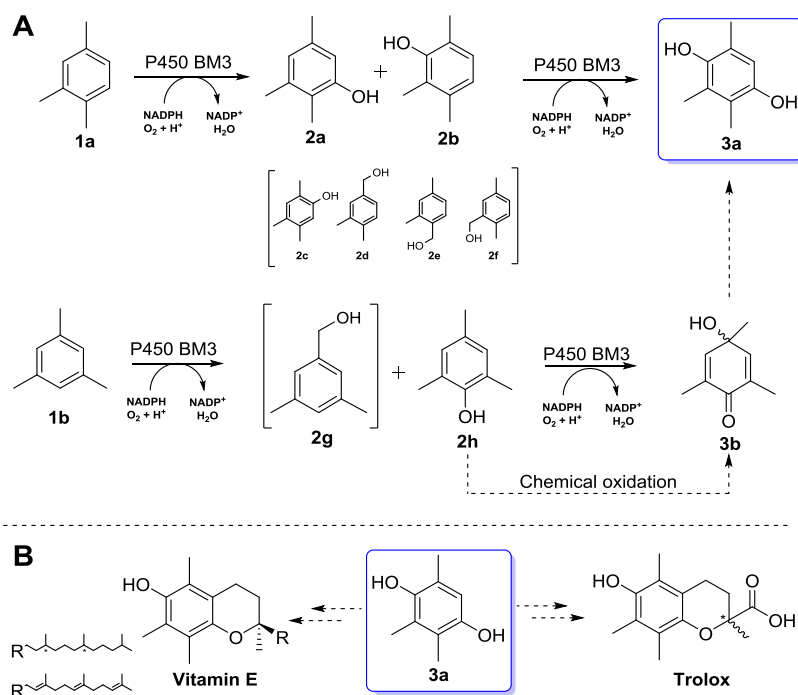
**KEYWORDS:** monooxygenase, protein engineering, phenol, tocopherol, aromatic hydroxylation, directed evolution.

## Introduction

The selective hydroxylation of non-activated C-atoms with O<sub>2</sub> remains a synthetic challenge in organic chemistry.<sup>[1]</sup> Industrial synthesis of phenol from benzene is inefficient and mainly proceeded via the multi-step cumene process (Hock synthesis, ~5% yield on benzene).<sup>[2]</sup> A vast number of pharmaceuticals, plastics, resins and vitamins<sup>[2b, 3]</sup> contain phenolic moieties making this class of compounds indispensable in everyday life. Industrially important alkylphenols can be obtained via phenol methylation<sup>[4]</sup> or chlorination followed by hydrolysis<sup>[5]</sup> requiring at least three synthetic steps starting from benzene. Trimethylphenols (TMPs) represent key synthons for  $\alpha$ -tocopherols and  $\alpha$ -tocotrienols (vitamin E), which find broad applications as anti-oxidants, dietary supplements, UV-protectors, anti-tumor or anti-inflammatory agents.<sup>[3b, 3c, 6]</sup> Natural sources of vitamin E do not cover the annual demand (>30000 tons per year).<sup>[3b]</sup> In particular, the most potent form of vitamin E, namely (2'R,4'R,8'R)- $\alpha$ -tocopherol, can only be extracted in racemic form from natural resources, which makes innovative synthesis inevitable.<sup>[3c, 6c]</sup> Chemical synthesis of  $\alpha$ -tocopherol precursors such as 2,3,5- or 2,3,6-TMP (**2a** and **2b**, Scheme 1) was summarized in an excellent and detailed review.<sup>[3b]</sup> Synthesis of **2a** and **2b** requires typically three or more steps including purification of intermediates. Alternatively, Pd-catalysts and high temperatures (350 °C) allow electrophilic acylation of 2,3-xyleneol to yield **2a**.<sup>[7]</sup> Only a few chemical routes were reported for the direct synthesis of **2a** or **2b** from pseudocumene (**1a**).<sup>[6b, 8]</sup> These routes often require either transition metal catalysts and/or strong oxidizing agents such as trifluoroperacetic acid. Due to low selectivity of the reaction, formation of unwanted side products such as quinones, mesitol or 2,4,5-TMP occurs. **2a** and **2b** can further be oxidized to yield trimethylhydroquinone (TMHQ, **3a**), the central phenol building block for vitamin E (Scheme 1B).<sup>[3b, 6b, 9]</sup> Another route starts from mesitol (2,4,6-TMP; **2h**, Scheme 1A), which after oxidation and rearrangement yields **3a**.<sup>[3b]</sup> **2h** can also be obtained in good yields from

mesitylene (**1b**) using a Re-catalyst and explosive concentrations of H<sub>2</sub>O<sub>2</sub> (85%)<sup>[10]</sup> or via application of strong acids and expensive bis(trimethylsilyl) peroxide.<sup>[11]</sup> Just recently, Lindhorst et al. could show oxidation of **1a** with an iron–heterocyclic carbene complex and H<sub>2</sub>O<sub>2</sub> as the oxidant, thus yielding a mixture of various phenols and benzoquinones.<sup>[6b]</sup> The increasing demand for phenolics and the usually harsh reaction conditions and low selectivity during chemical hydroxylation underlines the importance to explore alternative synthetic routes.<sup>[2b, 9]</sup> Ideally, a novel synthetic route should provide high efficiency, selectivity, and also sustainability.<sup>[3c]</sup> The selective aromatic hydroxylation under mild reaction conditions with either O<sub>2</sub> or H<sub>2</sub>O<sub>2</sub> as oxidant can be catalyzed by iron- or copper-containing proteins such as mono- and dioxygenases<sup>[2a, 12]</sup>, peroxygenases<sup>[13]</sup> or tyrosinases.<sup>[12b]</sup> However, most enzymes lack the required operational performance for industrial applications, including poor activities or low stability, jointly leading to low product yields.<sup>[1, 14]</sup> In two previous studies, we reported the engineering of the P450 monooxygenase BM3<sup>[12e]</sup> toward efficient and selective *o*-hydroxylation of mono-substituted benzenes<sup>[12a]</sup> and *p*-xylene.<sup>[2a]</sup> The catalyst was further applied in combination with a tyrosine phenol lyase for preparative synthesis of enantiopure L-tyrosine derivatives underlining its synthetic potential.<sup>[15]</sup> Site saturation mutagenesis of residue F87 proved that the phenylalanine in the active site provides indispensable interactions for efficient aromatic hydroxylation of benzenes.<sup>[12a]</sup> Based on experimental results and substrate docking, a tight  $\pi$ - $\pi$  interaction of residue F87 and anisole as ligand was postulated.<sup>[12a, 12c]</sup> Despite that  $\alpha$ -hydroxylation (hydride-abstraction followed by hydride-rebound)<sup>[12e, 16]</sup> and aromatic hydroxylation (aryl epoxidation followed by NIH-shift and re-aromatization)<sup>[12c, 17]</sup> require different steps in the P450 reaction mechanism, the active site of P450 BM3 precisely directs the substrate to achieve highly regio- and chemo-selective conversion of a broad range of benzenes.<sup>[2a, 12a, 12c, 12d, 15, 18]</sup> Encouraged by these results, we decided to extend our investigations to the aromatic hydroxylation of sterically more demanding benzenes such as **1a** and **1b**, which to date were only hydroxylated

(enzymatically) on benzylic positions e.g. employing xylene monooxygenases.<sup>[19]</sup> We emphasized in particular on the synthesis of **2a**, **2b**, and **2h**, which can serve as starting materials for the production of antioxidants or antitumor agents such as the water soluble vitamin E analogue Trolox (Scheme 1B).<sup>[20]</sup>



**Scheme 1. A:** Hydroxylation of pseudocumene (**1a**) with P450 BM3 yields 2,3,5- and 2,3,6-trimethylphenol (**2a**, **2b**). Additional side products (**2c-2f**) formed during conversion of **1a** are highlighted in brackets. Further hydroxylation enables synthesis of trimethylhydroquinone (TMHQ, **3a**) in one-pot mode. Hydroxylation of mesitylene (**1b**) with P450 BM3 yields 2,4,6-TMP (**2h**). Further hydroxylation of **2h** yields **3b** (4-hydroxy-2,4,6-trimethylcyclohexa-2,5-dien-1-one).<sup>[21]</sup> **B:** **3a** represents the central aromatic precursor for synthesis of vitamin E or the water-soluble anti-oxidant Trolox.<sup>[3b]</sup> NADP(H) = Nicotinamide adenine dinucleotide phosphate.

Direct enzymatic hydroxylation of **1a** or **1b** would be advantageous and open novel and greener routes to industrially relevant alkyl-phenols.

## Results and Discussion

### Conversion of **1a** and **1b** with P450 BM3 WT and variants M1 and M2

Catalytic characterization of P450 BM3 for conversion of **1a** and **1b** was done measuring NADPH oxidation rates and product formation by GC-FID/-MS with authentic standards (see SI). The P450 BM3 WT hydroxylates **1a** and **1b** at very low turnover frequencies (TOFs) of 3.2 and 0.3 min<sup>-1</sup>, respectively (Table 1, entry 1 and 4). Measured productivities correlate with the low NADPH oxidation rates of P450 BM3 WT (**1a** = 22 min<sup>-1</sup>; **1b** = 13 min<sup>-1</sup>), indicating that both substrates do not enter efficiently the active site of the monooxygenase to initiate the catalytic cycle.<sup>[12e, 16-17]</sup> The two polar amino acid residues R47 and Y51 ('gate keepers')<sup>[12e]</sup> often hinder sterically demanding substrates to efficiently enter the substrate channel of P450 BM3.<sup>[2a, 12a, 18b, 18c]</sup> In addition, a very low coupling efficiency of only 3% for **1b** indicates a loose-fitting in the active site<sup>[22]</sup>, possibly due to higher sterical demands as compared to *p*-xylene (45%)<sup>[2a]</sup> or toluene (10%).<sup>[12a]</sup> Unexpectedly and despite of the low catalytic activity, a total turnover number (TTN) of 1602 (Table 2, entry 2) could be measured for hydroxylation of **1a** using cell free extracts (CFE) of P450 BM3 WT and a glucose dehydrogenase (GDH) for NADPH recycling.<sup>[15, 23]</sup> A TTN >1500 at only 15% coupling efficiency (Table 1, entry 1) is a good value and still one order of magnitude higher than TTNs of most chemical catalysts used for oxyfunctionalization.<sup>[6b, 24]</sup> A comparable chemical catalyst (1% loading) showed after reaction optimization 54 turnover cycles for conversion of **1a** using H<sub>2</sub>O<sub>2</sub> as oxidant.<sup>[6b]</sup> For conversion of **1b** a TTN of only 393 was determined, which is 4-fold lower than for **1a** and can be explained by the significant lower coupling efficiency (3%; 5-fold lower; Table 1, entry 4). A low coupling efficiency often results in formation of reactive oxygen species such as H<sub>2</sub>O<sub>2</sub> or O<sub>2</sub><sup>-</sup> that can lead to rapid catalyst inactivation.<sup>[22b, 25]</sup> Chemoselectivity of P450 BM3 WT for **1b** is preferentially toward the aromatic ring leading to formation of **2h** (83%; Table 2, entry 11), which is in good agreement with other reports on

structural related benzene substrates (e.g. *m*-xylene).<sup>[2a, 12a, 15, 18c]</sup> 3,5-dimethylbenzylalcohol (**2g**) was detected only in traces (6%). In contrast, P450 BM3 WT converted **1a** to all theoretically possible mono-hydroxylated products (**2a-2f**; Table 2, entry 1 and 2). A low chemoselectivity of P450 BM3 WT for aromatic hydroxylation of *o*-xylene (45%) as compared to *p*-xylene (>95% *o*-hydroxylation) and *m*-xylene (98%) has been shown before.<sup>[2a, 18b]</sup> Major products during conversion of **1a** with P450 BM3 WT are 2,4-DMBA (**2e**; 40%), 2,4,5-TMP (**2c**; 23%) and 2,5-DMBA (**2f**; 21%), in summary 84% (Table 2, entry 1). Secondary hydroxylation products of **1a** were obtained in traces (3%) and only in presence of a cofactor regeneration system (Table 2, entry 2). To overcome the drawbacks of P450 BM3 WT, we decided to employ P450 BM3 variant M2 (R47S, Y51W, I401M) as catalyst, which was engineered for aromatic hydroxylation of *p*-xylene.<sup>[2a]</sup> Compared to the P450 BM3 WT, variant M2 displayed improved hydroxylation of **1a** and **1b** (Table 1). P450 BM3 variant M2 displayed a 2.6-fold higher NADPH oxidation rate during conversion of **1b**, resulting overall in a 4.7-fold higher TOF (1.4 min<sup>-1</sup>; Table 1, entry 5) as compared to the P450 BM3 WT. Despite this improvement, the productivity remained very low and more than three orders of magnitude lower as compared to *p*-xylene (1953 min<sup>-1</sup>)<sup>[2a]</sup> or anisole (2427 min<sup>-1</sup>).<sup>[12a]</sup> Differences in substrate solubility could play an important role; in particular in case of anisole, which is 3900-fold more soluble in water (1.85 mol L<sup>-1</sup>)<sup>[26]</sup> than **1a** (0.4 μmol L<sup>-1</sup>).<sup>[27]</sup> Regioselectivity of P450 BM3 variant M2 remained high for aromatic hydroxylation of **1b** yielding 89% of **2h** (Table 2, entry 11). Minor changes in chemoselectivity and coupling efficiency indicate a similar orientation of **1b** in the active site of P450 BM3 WT and variant M2 (no active site residue with direct substrate interaction exchanged).<sup>[2a]</sup> Conversion of **1a** with P450 BM3 variant M2 displayed a 4-fold improved NADPH depletion rate (87 min<sup>-1</sup>) as well as an increased coupling efficiency by 4% (Table 1, entry 2). Still, a TOF of only 17 min<sup>-1</sup> is a comparably low value for benzene conversion with P450 BM3.<sup>[2a, 12a, 18b, 18c]</sup> Chemoselectivity during conversion of **1a** by P450 BM3 variant M2 was shifted toward

increased aromatic hydroxylation and accumulation of an additional product was detected when a cofactor regeneration system was applied. The product was after preparative isolation and comparison with a commercial standard identified as TMHQ (**3a**, 32%, for  $^1\text{H-NMR}$  analysis see SI). Major products after conversion of **1a** with purified P450 BM3 variant M2 are 2,4-DMBA (**2e**, 25%) and 2,4,5-TMP (**2c**, 39%) (Table 2, entry 5). To investigate the influence of the two mutations at the entrance of the substrate channel (residues 47 and 51), we decided to use also the P450 BM3 variant M1 (R47S, Y51W)<sup>[2a]</sup> for conversion of **1a**. P450 BM3 variant M1 displayed similar regioselectivity as compared to P450 BM3 WT, while TTN values could be improved significantly from 1602 to 4910 (Table 2, entry 2 vs. 4).

**Table 1.** Catalytic data for conversion of **1a** and **1b** with purified P450 BM3 enzymes.

Entry	Substrate	Catalyst	NADPH ox. rate [ $\text{min}^{-1}$ ] <sup>[a]</sup>	Coupling [%] <sup>[b]</sup>	TOF [ $\text{min}^{-1}$ ] <sup>[c]</sup>
1	<b>1a</b>	WT	22 ± 4	15 ± 2	3.2
2	<b>1a</b>	M2	87 ± 3	19 ± 2	17
3	<b>1a</b>	M3	499 ± 91	45 ± 6	226
4	<b>1b</b>	WT	13 ± 2	3 ± 1	0.3
5	<b>1b</b>	M2	34 ± 14	4 ± 2	1.4
6	<b>1b</b>	M3	285 ± 20	24 ± 2	69

[a] NADPH oxidation rate ( $\text{mol}_{\text{cofactor}} \text{mol}_{\text{P450}}^{-1} \text{min}^{-1}$ ) was determined spectrophotometrically at 340 nm absorbance; [b] Coupling efficiency (%) = ratio between product formation [ $\mu\text{M}$ ] and oxidized cofactor [ $\mu\text{M}$ ]; [c] Turnover frequency ( $\text{mol}_{\text{product}} \text{mol}_{\text{P450}}^{-1} \text{min}^{-1}$ ). **WT** = P450 BM3 wild type; **M2** = P450 BM3 mutant (R47S, Y51W, I401M)<sup>[2a]</sup>; **M3** = P450 BM3 mutant (R47S, Y51W, I401M, A330F) (obtained in this study). Conversions were done using purified P450 BM3 protein (0.3  $\mu\text{M}$  WT enzyme or 0.1  $\mu\text{M}$  for the P450 BM3 variants), 10 mM substrate (**1a** or **1b**), 1.5% DMSO as co-solvent in a final volume of 5 mL. 200  $\mu\text{M}$  NADPH were added and the activity of P450 BM3 was measured as initial NADPH oxidation rates at 340 nm. Products were quantified using GC-FID and commercial standards for **2a-h**.

Under continuous NADPH regeneration, P450 BM3 variant M2 displayed even a higher TTN of 5268 (3.3-fold increase compared to P450 BM3 WT) for conversion of **1a** (Table 2, entry 6). For conversion of **1b** with CFE of P450 BM3 variant M2 a TTN of 1243 was measured which is a 3.2-fold improvement compared to P450 BM3 WT (Table 2). A higher coupling

efficiency (Table 1), the improved electron transfer/O<sub>2</sub> activation (substitution I401M)<sup>[2a, 12a]</sup> and a better access of the substrate to the active site (substitutions R47S and Y51W)<sup>[2a, 12a, 12e, 18b, 18c]</sup> jointly improve the catalytic performance of P450 BM3 variant M2 for conversion of **1a** and **1b**.

### Engineering P450 BM3 toward improved conversion of **1a**

In order to improve the catalytic performance (activity and coupling efficiency) of P450 BM3 variant M2, the position A330 was, after structural inspection, mutated using P450 BM3 variant M2 as template followed by screening for improved hydroxylation of **1a** (see SI). Position 330 was previously reported to influence the activity of P450 BM3 for aromatic hydroxylation of toluene and ethyl benzene.<sup>[18c]</sup> Further it could be shown that rational introduction of a proline on position 330 (A330P) led to relocation of a neighboring proline (P329) toward the substrate binding pocket resulting in higher coupling efficiency and activity of P450 BM3.<sup>[18c]</sup> Here, position 330 was saturated to all 20 canonical amino acids and screened for improved NADPH oxidation (**1a** as substrate). Using **1a** as substrate allows formation of the target products **2a** and **2b**, which are easily detectable in microtiter plate (MTP) format by the colorimetric 4-AAP assay.<sup>[28]</sup> A high number of improved variants (76%) were identified within the generated library (see SI; 180 variants screened; theoretical calculated >95% diversity coverage).<sup>[29]</sup> This indicates that the P450 BM3 WT active site configuration (and in particular residue A330) reduces the efficient binding and conversion of **1a** (Table 1). The best three P450 BM3 muteins (based on phenol production; see SI) contained each a phenylalanine at position 330 (A330F) which is, to the best of our knowledge, an unreported amino acid exchange in P450 BM3.<sup>[12e]</sup> One variant (herein named P450 BM3 variant M3 = R47S, Y51W, A330F, I401M) was selected for purification and detailed catalytic characterization. P450 BM3 variant M3 displayed a 22-fold higher NADPH oxidation rate during conversion of **1b** than P450 BM3 WT and a 8.4-fold higher rate than

P450 BM3 variant M2, respectively (Table 1; Entry 4-6). Moreover, an improved productivity (TOF = 226 min<sup>-1</sup>) was measured during conversion of **1a**. For both substrates the coupling efficiency was increased (24% for **1b**; 45% for **1a**) in the range of 2- to 6-fold as compared to P450 BM3 variant M2 (Table 1). The latter is in good agreement with the results obtained during activity screenings in MTP format. When comparing TOF values for **1b**, P450 BM3 variant M3 is a 230-fold better hydroxylase than the P450 BM3 WT and 49-fold better than P450 BM3 variant M2, respectively (Table 1). In case of **1a**, the improvements range from 13-fold compared to P450 BM3 variant M2 and 71-fold compared to P450 BM3 WT. Selectivity of P450 BM3 variant M3 remained high for aromatic hydroxylation of **1b** (89-94%, Table 2, entries 13 and 14). In case of **1a**, minor changes in product distribution were detected (Table 2) as compared to P450 BM3 variant M2. In presence of a NADPH regeneration system, P450 BM3 variant M3 (applied as CFE) reached a product concentration of up to 0.48 g L<sup>-1</sup> (mixture of **2a-2f**) for conversion of **1a**, which corresponds to a TTN of 4569. Conversion of **1b** with P450 BM3 variant M3 showed an increase in TTN (19% vs. P450 BM3 variant M2) underlining the overall improved operational performance. Higher TOF values were (as a general trend) obtained for conversion of **1a** as compared to **1b** (Table 1; entry 1-3 vs. entry 4-6). This indicates that only small structural differences can lead to dramatic changes in selectivity, coupling efficiency and activity, which has been shown for conversion of xylene isomers.<sup>[2a, 18b]</sup> In addition to **1a** and **1b**, we also investigated the hydroxylation of anisole and toluene with P450 BM3 variant M3 (CFE as catalyst supported by a GDH cofactor regeneration system). Selectivity of P450 BM3 variant M3 for hydroxylation of *o*-positions remained very high for both substrates (95-99%)<sup>[12a]</sup>, whereas the TTN values could be further increased (anisole: 8536; toluene: 6262) as compared to P450 BM3 variant M2 (anisole: 6195; toluene 3740)<sup>[12a]</sup> making P450 BM3 variant M3 an overall better catalyst for aromatic hydroxylation of benzenes. It is worth mentioning that for

anisole/toluene secondary hydroxylation to the respective 1,4-hydroquinones occurred as reported before.<sup>[15, 30]</sup>

**Table 2.** Selectivity and productivity of P450 BM3 WT and variants using cell-free extracts (CFE) or purified enzymes.

Entry	Substrate	Conv. [%]	Catalyst	2a-2c [%]	2d-2f [%]	3a [%]	2a-c:2d-f:3a [%]	TTN [-]
1	<b>1a</b>	---	WT	9/4/23	3/40/21	0	36:64:0 <sup>[a]</sup>	---
2	<b>1a</b>	16	WT <sub>cf</sub>	8/9/34	5/27/14	3	51:46:3	1602
3	<b>1a</b>	---	M1	3/5/34	3/37/18	0	42:58:0 <sup>[a]</sup>	---
4	<b>1a</b>	44	M1 <sub>cf</sub>	4/5/34	2/31/12	12	43:45:12	4910
5	<b>1a</b>	---	M2	6/17/39	2/25/11	0	62:38:0 <sup>[a]</sup>	---
6	<b>1a</b>	40	M2 <sub>cf</sub>	7/4/31	2/17/7	32	42:26:32	5268
7	<b>1a</b>	---	M3	6/14/41	1/29/9	0	61:39:0 <sup>[a]</sup>	---
8	<b>1a</b>	34	M3 <sub>cf</sub>	7/4/29	2/17/6	35	40:25:35	4569
9 (10 mL)	<b>1a</b>	29	M3 <sub>cf</sub>	8/5/28	2/25/9	23	41:36:23	3528
10	<b>2a/2b</b>	42/49	M3 <sub>cf</sub>	---	---	>99/>99	-	4225/4978
Entry	Substrate	Conv. [%]	Catalyst	2g [%]	2h [%]	3b [%]	2g:2h:3b [%]	TTN [-]
11	<b>1b</b>	1	WT	6	83	11	6:83:11	395
12	<b>1b</b>	4	M2	3	89	8	3:89:8	1242
13	<b>1b</b>	5	M3	4	85	11	4:85:11	1526
14 <sup>[b]</sup> (50 mL)	<b>1b</b>	>99	M3 <sub>cf</sub>	11	89	n.d.	11:89:n.d.	n.d.
15 <sup>[b]</sup> (1 mL)	<b>2h</b>	45	M3 <sub>cf</sub>	---	45	44	0:45:44	n.d.
16 <sup>[c]</sup> (100 mL)	<b>2h</b>	89	M3 <sub>cf</sub>	---	11	89	0:11:89	n.d.

**WT** = P450 BM3 WT. **M1** = P450 BM3 (R47S, Y51W)<sup>[2a]</sup>; **M2** = P450 BM3 (R47S, Y51W, I401M)<sup>[2a]</sup>; **M3** = P450 BM3 (R47S, Y51W, A330F, I401M). Selectivity/productivity was determined with commercial standards of **2a-h** and **3a**. Selectivity of purified enzymes and CFE are shown to report values under cofactor limited/unlimited conditions. Conversions with purified P450 BM3 protein (entries 1,3,5,7 and 11-13; 0.3 μM P450 BM3 WT or and 0.1 μM for the P450 BM3 variants) contained: 10 mM **1a/1b**, 1.5% DMSO as co-solvent in a final volume of 5 mL. 200 μM NADPH (final concentration) was added to start the reaction. Reaction conditions for entries 2,4,6,8 and 9: 10 mM substrate, 2% DMSO, CFE (1 μM P450 BM3 WT or variants), GDH cofactor regeneration system. All reactions (except for entry 13 and 15) were done in triplicate. [a] Secondary hydroxylations did not occur in these reactions due to limited amount of NADPH. [b] Reaction contained: 4 mM **1b**, 30 mg of freeze dried CFE of variant M3, GDH-cofactor regeneration system. [c] Reaction was done under continuous pH control and with pressurized air constantly supplied from top into the glass flask, which leads to significant evaporation of **2g** (no substrate recovered after extracting with organic solvent). Further experimental details and analytical data of isolated compounds can be found in SI. n.d. = not determined.

### One-pot double-hydroxylation of **1a** and **1b**

In the presence of a co-factor regeneration system, secondary hydroxylation of **1a** and **1b** were detected by GC-FID/MS. In case of **1b** over-oxidation leads to formation of the *p*-quinol 4-hydroxy-2,4,6-trimethylcyclohexa-2,5-dien-1-one (**3b**), a versatile building block for natural products, therapeutics and organic synthesis in general.<sup>[21]</sup> Beneficially, **3b** can further serve as intermediate for synthesis of **3a**<sup>[3b]</sup> which was not detected during conversion of **1b/2h**. For detailed compound analysis and identification, **3b** was produced on 50 mL scale using **2h** as substrate (10 mM; P450 BM3 variant M3 as catalyst). After isolation and purification (11 mg isolated) the product was analyzed using <sup>1</sup>H-/<sup>13</sup>C-NMR and GC-MS and compared to literature values (see SI).<sup>[21]</sup> Despite a huge industrial interest in **2h** (~90 patent applications)<sup>[31]</sup> there has been (to the best of our knowledge) no biocatalytic route described showing conversion of **1b** into **2h** or **3b**. In case of **1a**, the over-oxidation of **2a** and/or **2b** enables the direct/linear synthesis of **3a** without the need for additional catalysts/reactants or intermediate isolation (Scheme 1A). The formation of **3a** in the reactions using **1a**, (or **2a/2b**) as substrate revealed that all P450 BM3 enzymes are able to produce the desired vitamin E synthon. Employing P450 BM3 WT for conversions of **1a** generates **3a** only in traces (<0.01 g L<sup>-1</sup>), whereas P450 BM3 variant M1 displayed an 8-fold increased product formation of up to 0.08 g L<sup>-1</sup> of **3a**. Conversion of **1a** with P450 BM3 variants M2 and M3 revealed further increased selectivity (up to 32-35%; one-pot conversion of **1a**) for **3a** (P450 BM3 variant M2 = 0.19 g L<sup>-1</sup>; P450 BM3 variant M3 = 0.1 to 0.18 g L<sup>-1</sup>; Table 2 entry 8 and 9). Starting from **2a** or **2b**, P450 BM3 variant M3 generated (without additional reaction optimization) even higher product concentrations for **3a** (0.64 g L<sup>-1</sup> and 0.76 g L<sup>-1</sup>; Table 2, entry 10; >99% selectivity). To prevent rapid oxidation of **3a** to the respective 1,4-benzoquinone, all conversions were performed in presence of 10 mM ascorbic acid (weak/mild reducing agent),

which had no detrimental effect on the biocatalysts. In order to analyze the diverse product patterns obtained from secondary hydroxylation of **1a**, all six mono-hydroxylated products (**2a-f**) were converted separately by P450 BM3 variant M3. Since the formation of **3a** (major double hydroxylated product) would be expected to proceed via **2a** and **2b** hydroxylation (excluding methyl group shifts), we determined NADPH oxidation rates using both compounds as substrates. For **2a/2b** a significantly higher NADPH oxidation rate was measured as compared to **2c-f** and **1a** (see SI); the latter indicates that hydroxylation of **2a** and **2b** is favored and high selectivity (>99%) drives the reaction efficiently toward formation of **3a**. During conversions of **1a** additional di-hydroxylated products could be detected, which were most likely derived from conversion of **2c** and **2e** (see SI). Secondary hydroxylation of substrates is usually unwanted and requires careful adjustment of the reaction system<sup>[15]</sup> or further catalyst engineering. For accessing the vitamin E synthons **3a/3b**, the observed over-oxidations of phenolic intermediates are desirable since intermediate work-up or additional catalysts/reagents are not required.<sup>[3b]</sup>

### Substrate binding and chemo-selectivity of P450 BM3

Computational assisted docking studies (using YASARA software package)<sup>[32]</sup> were performed to generate a molecular understanding of achieved improvements in activity, coupling efficiency (Table 1), and altered chemoselectivity (Table 2). Docking of substrates provides binding modes during catalysis, which can be described by the Gibbs free energy of binding ( $\Delta G_{\text{bind}}$ ).<sup>[33]</sup> Docking was performed using **1a** and **1b** as ligand and the crystal structure of P450 BM3 WT was employed as receptor molecule (PDB: 1BU7).<sup>[34]</sup> In addition, a homology model structure of P450 BM3 variant M3 was generated for docking of both substrates. It is well accepted for P450-catalyzed reactions that a close interaction of the substrate and the heme-bound water ligand is essential to initiate the catalytic cycle<sup>[17]</sup>, whereas a strong binding of a potential substrate allows a high coupling efficiency.<sup>[22b]</sup>

Herein, only substrate orientations are shown that correspond to productive binding modes<sup>[32, 33b]</sup> and which are in agreement with catalytic data (Table 1 and 2). Docking of **1b** into the active site of the P450 BM3 WT revealed one binding mode that allows equally  $\alpha$ -benzylic hydroxylation or 1,2-epoxidation of aryllic carbons (Figure 1A)<sup>[17, 18b]</sup> and formation of the major product **2h** (Table 2, entries 10 to 12).

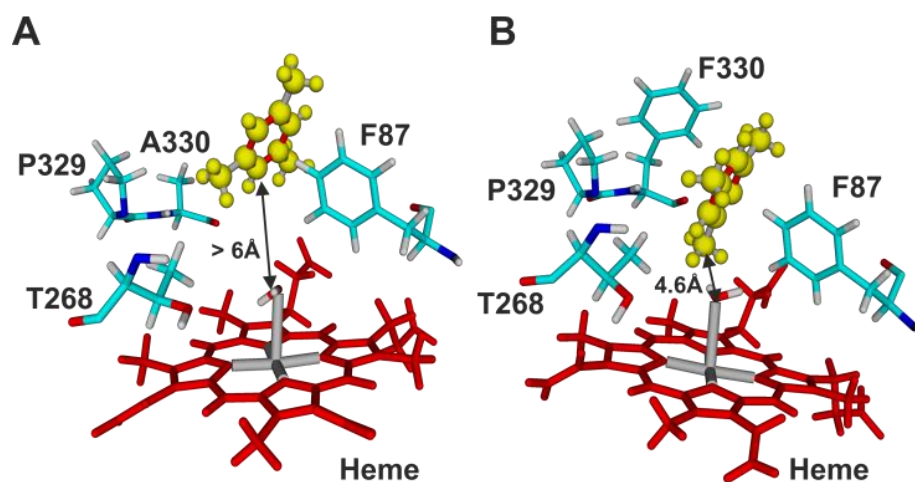


**Figure 1.** Docking of **1b** into the active site of P450 BM3 WT and the homology model of P450 BM3 variant M3.<sup>[32, 33b]</sup> **A:** **1b** docked into the crystal structure model of P450 BM3 WT (1BU7)<sup>[34]</sup> yielding either **2g** or **2h** ( $\Delta G_{\text{bind}}$ :  $-4.93 \text{ kcal mol}^{-1}$ ). **B:** Docking of **1b** into the active site of P450 BM3 variant M3 (R47S, Y51W, A330F, I401M;  $\Delta G_{\text{bind}}$ :  $-5.74 \text{ kcal mol}^{-1}$ ). Arrows indicate the closest distance between heme-bound water ligand and closest aryllic C-atoms of **1b**.

The binding of **1b** is comparably strong with  $-4.93 \text{ kcal mol}^{-1}$ <sup>[35]</sup>, however the distance between the water ligand and the closest C-atom exceeds  $6 \text{ \AA}$  suggesting a slow activation<sup>[12e, 16]</sup> that was determined experimentally for P450 BM3 WT (Table 1, Entry 4). Docking of **1b** into the homology model of P450 BM3 variant M3 (Figure 1B) suggested not only a stronger binding ( $\Delta G_{\text{bind}}$ :  $-5.74 \text{ kcal mol}^{-1}$ ), but also a closer distance to the water ligand ( $4.6 \text{ \AA}$ ). The closer and stronger binding is in good agreement with the measured improvements (higher

coupling and higher PFR for P450 BM3 variant M3; Table 1, entry 6) during conversion of **1b**. Both binding modes (P450 BM3 WT and variant M3) suggest equal hydroxylation of  $\alpha$ -benzylic and aromatic carbons (Figure 1). However, hydroxylation of **1b** proceeded preferentially at aryl positions (94 to 96%; Table 2), which opens the question how chemoselectivity during hydroxylation of aromatic compounds is directed by P450 BM3. One reason for the high selectivity could be that 1,2-epoxidation and re-aromatization is faster or more efficient than hydride-rebounding via compound II that requires also more catalytic steps<sup>[16-17]</sup> including formation of a carbon radical at the  $\alpha$ -position (Scheme 2B). Bond dissociation energies (BDE) of benzylic C-H bonds are similar for toluene (89 kcal mol<sup>-1</sup>) and **1b** (88 kcal mol<sup>-1</sup>)<sup>[36]</sup> and generally lower than for secondary aliphatic carbons (95 kcal mol<sup>-1</sup>), the preferred hydroxylation target for P450 BM3.<sup>[12e]</sup> However, it is on the molecular level unknown why P450 BM3 WT prefers aromatic over benzylic hydroxylation for most benzenes<sup>[2a, 12a, 12c, 15, 18b, 37]</sup> (Table 2; BDEs for benzylic H-bonds of *o*-, *m*-, *p*-xylene are 74, 81 and 71 kcal mol<sup>-1</sup>).<sup>[38]</sup> Previous investigations could not elucidate the reason on the enzyme's chemoselectivity during alkyl-benzene conversions. A common pattern throughout literature on alkyl-benzene hydroxylation with P450 BM3 is, that whenever a primary benzylic carbon has no *o*-substituent e.g. toluene, *p*-xylene, *m*-xylene or **1b** (as opposed to *o*-xylene and **1a**; both yield significantly higher amount of benzylalcohols) and P450 BM3 retains active site residue F87, aromatic *o*-hydroxylation is the predominant reaction with selectivity >95%.<sup>[2a, 12a, 12c, 15, 18b]</sup> Substituting F87 by alanine (removing  $\pi$ - $\pi$  interactions) leads to increased formation of benzylalcohols (45-83% for *m*-xylene and 94-99% for *o*-xylene)<sup>[18b]</sup> and a significant decrease in aromatic hydroxylation of *p*-xylene.<sup>[2a]</sup> Moreover decoy molecules can influence the formation of benzylalcohol slightly as shown for conversion of toluene in presence of five different perfluorinated fatty acids (5-8% benzyl alcohol formed, P450 BM3 WT).<sup>[12c]</sup>

Due to its non-symmetrical structure, the docking of **1a** is more complex and complexity rises due to the formation of six different mono-hydroxylated products (**2a-f**; Table 2). The conversion of **1a** by P450 BM3 WT leads predominantly to benzylalcohol formation (main products are **2e** and **2f**, 61%, Table 2; entry 1). On the other hand,  $\alpha$ -benzylic hydroxylation of **1a** at position 4 (no *o*-substituent on position 3 or 5) occurs with  $\leq 5\%$  **2d** formed (Table 2). Interestingly, this was independent of the P450 BM3 catalyst and supports the hypothesis of an *o*-CH<sub>3</sub> directed  $\alpha$ -hydroxylation. Docking of **1a** into the P450 BM3 WT structure proposes three major orientations with strong binding energies (Figure 2; A:  $-5.60$  kcal mol<sup>-1</sup>; B:  $-5.53$  kcal mol<sup>-1</sup>; C:  $-5.37$  kcal mol<sup>-1</sup>) as well as a comparably close distance of **1a** to the heme-bound water ligand (Figure 2; A: 3.37 Å; B: 3.34 Å; C: 3.01 Å).

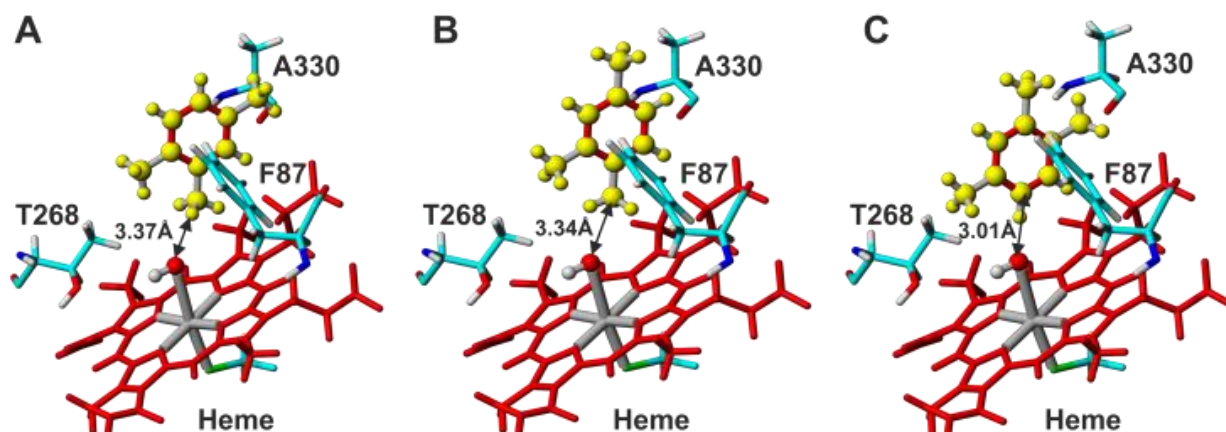


**Figure 2.** Docking of **1a** into the active site of P450 BM3 WT (1BU7).<sup>[34]</sup> **A:** Binding orientation ( $\Delta G_{\text{bind}}$  of  $-5.60$  kcal mol<sup>-1</sup>) allowing hydroxylation preferentially at the  $\alpha$ -benzylic C-2 (product: **2f**). **B:** Binding orientation ( $\Delta G_{\text{bind}}$  of  $-5.53$  kcal mol<sup>-1</sup>) allowing  $\alpha$ -hydroxylation preferentially at  $\alpha$ -benzylic C-1 (product: **2e**). **C:** Binding orientation ( $\Delta G_{\text{bind}}$  of  $-5.37$  kcal mol<sup>-1</sup>) allowing aromatic hydroxylation of **1a** (product: **2c**). Arrows indicate the closest distance between the heme-bound water ligand and C-atoms of **1a**.

This would allow a faster initiation of the catalytic cycle<sup>[16]</sup> as compared to **1b**, which was determined experimentally (Table 1). The three binding modes showed in Figure 2

preferentially lead to formation of **2f** (A), **2e** (B), and **2c** (C) which, after biochemical characterization, comprise in total 75 to 84% (Table 2, entry 1 and 2). We conclude that **1a** binds with high probability in the suggested modes. In the P450 BM3 WT crystal structure model docking, residue A330 does not directly interact with **1a** as the aliphatic side chain is pointing away from the substrate binding pocket (Figure 2, A-C). The unexpected high number of improved variants (76%, see SI) obtained after site-saturation mutagenesis of position 330, suggests that sterically more demanding amino acids (18 in total) provide interactions essentially for improved conversion of **1a** (Table 1). The homology model of P450 BM3 variant M3 places the best fitting rotamer of F330 toward the substrate binding pocket/substrate channel thus leading to additional and beneficial aromatic interaction(s) between amino acids F87/F330 and the benzene substrate.<sup>[35]</sup> **1a** docked into the homology model of P450 BM3 variant M3 yielded an even stronger binding of  $-6.33 \text{ kcal mol}^{-1}$  (Figure 3, A), whereas the distance between the closest C-atom and heme iron was increased ( $5.04 \text{ \AA}$ ) as compared to the P450 BM3 WT (Figure 2, A-C).

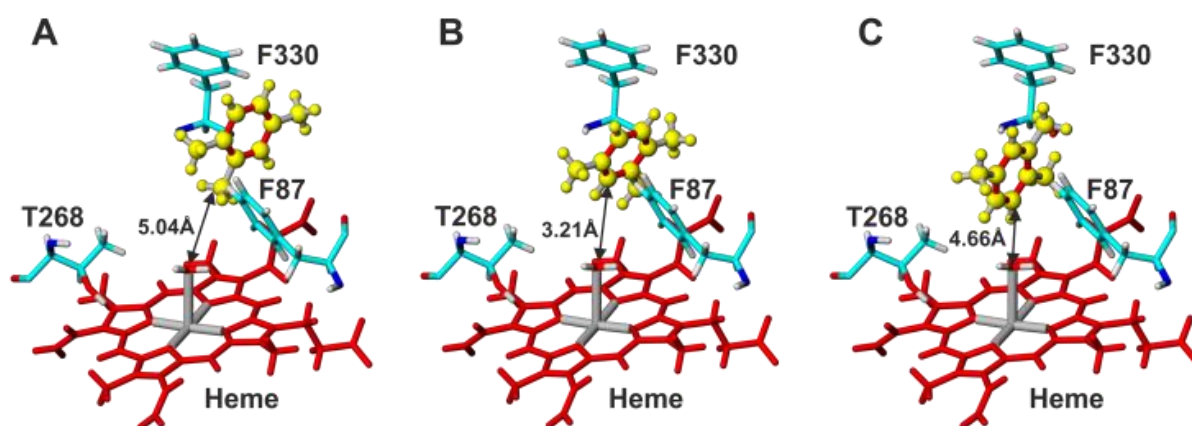


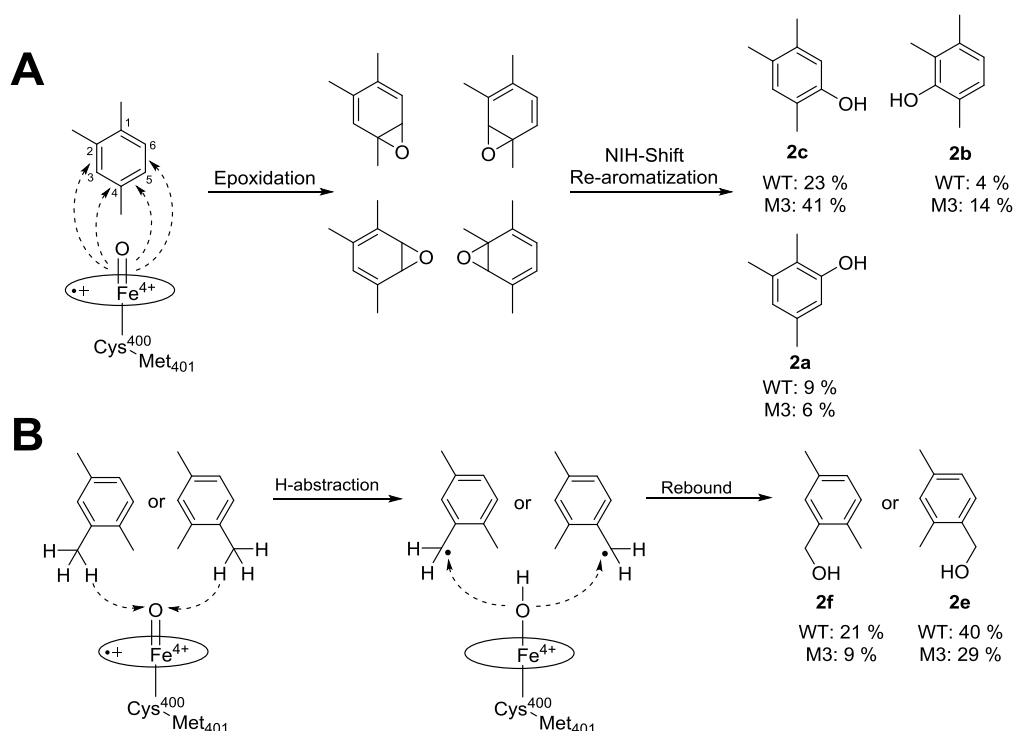
**Figure 3.** Docking of **1a** into active site of P450 BM3 variant M3 (R47S, Y51W, A330F, I401M). **A:** Binding orientation ( $\Delta G_{\text{bind}}$  of  $-6.33 \text{ kcal mol}^{-1}$ ) allowing hydroxylation of **1a** at the  $\alpha$ -benzylic C-1 (product: **2f**). **B:** Binding orientation ( $\Delta G_{\text{bind}}$  of  $-5.01 \text{ kcal mol}^{-1}$ ) allowing aromatic hydroxylation of **1a** (position C-3; product: **2b**). **C:** Binding orientation ( $\Delta G_{\text{bind}}$  of -

5.51 kcal mol<sup>-1</sup>) allowing aromatic hydroxylation at C-5 or C-6 (product: **2a** or **2c**). Arrows indicate the closest distance between heme-bound H<sub>2</sub>O ligand and the targeted C-atom of **1a**.

Orientation B (-5.53 kcal mol<sup>-1</sup>) represents the closest binding orientation of **1a** near the heme iron (3.21 Å) in P450 BM3 variant M3 suggesting the preferential formation of **2b**. The proposed binding mode is supported by an increased formation of **3a** (via **2a/2b** intermediates) in the GDH supported reactions as compared to P450 BM3 WT (Table 2, entry 2 and 8). Orientation C (Figure 3) binds **1a** with -5.51 kcal mol<sup>-1</sup> and a larger distance to the heme iron. This would in theory result in higher formation of **2a** or **2c**, of which at least **2c** was increased (entry 1 vs. entry 7; Table 2) as compared to the P450 BM3 WT. A previous docking of anisole into the active site of P450 BM3 WT was in good agreement with the measured selectivity as well as catalytic activity and generated the hypothesis of a T-shape orientation/interaction coordinated by active site residue F87.<sup>[12a]</sup> Binding modes A-C (Figure 3) suggest that **1a** is stacked between residues F330 and F87 in a T-shape  $\pi$ -**1a**- $\pi$  orientation (*aromatic sandwich*).<sup>[35]</sup> The semi-rationally introduced phenylalanine generates an even stronger substrate binding (as shown during docking; increased coupling efficiency for **1a/1b**) very likely through aromatic ( $\pi$ - $\pi$  stacking) interactions<sup>[35]</sup>, which improved conversion of **1a** and **1b** by variant M3 (Table 1).

Assuming the binding modes for **1a** (Figures 2 and 3) are in good correlation with the catalytic data, we analyzed product patterns and alterations in chemo-selectivity between P450 BM3 WT and variant M3. It is well accepted that aromatic hydroxylation of benzenes proceeds via epoxidation of the aromatic ring followed by epoxide ring opening, NIH-shift and re-aromatization to the respective phenol (Scheme 2A).<sup>[17, 18b, 37]</sup> In addition, methyl-group shifts were previously observed during conversion of *o*-xylene with P450 BM3.<sup>[18b]</sup> For conversion of **1a** and **1b** we did not observe CH<sub>3</sub>-shifts. Scheme 2 shows routes to the major phenolic and benzylic alcohol products detected after the conversion of **1a** with purified P450

BM3 WT and variant M3 (Table 2). When orienting the substrate with the aromatic carbon 4 (C-4) toward compound I, P450 BM3 variant M3 is able to catalyze 3,4- and 4,5-epoxidation of which the latter would yield **2c** as product (41%; Table 2, Entry 7; Scheme 2A). This orientation is also supported by an increased formation of **2b** and directly related to an increased formation of **3a** (35%, Table 2).



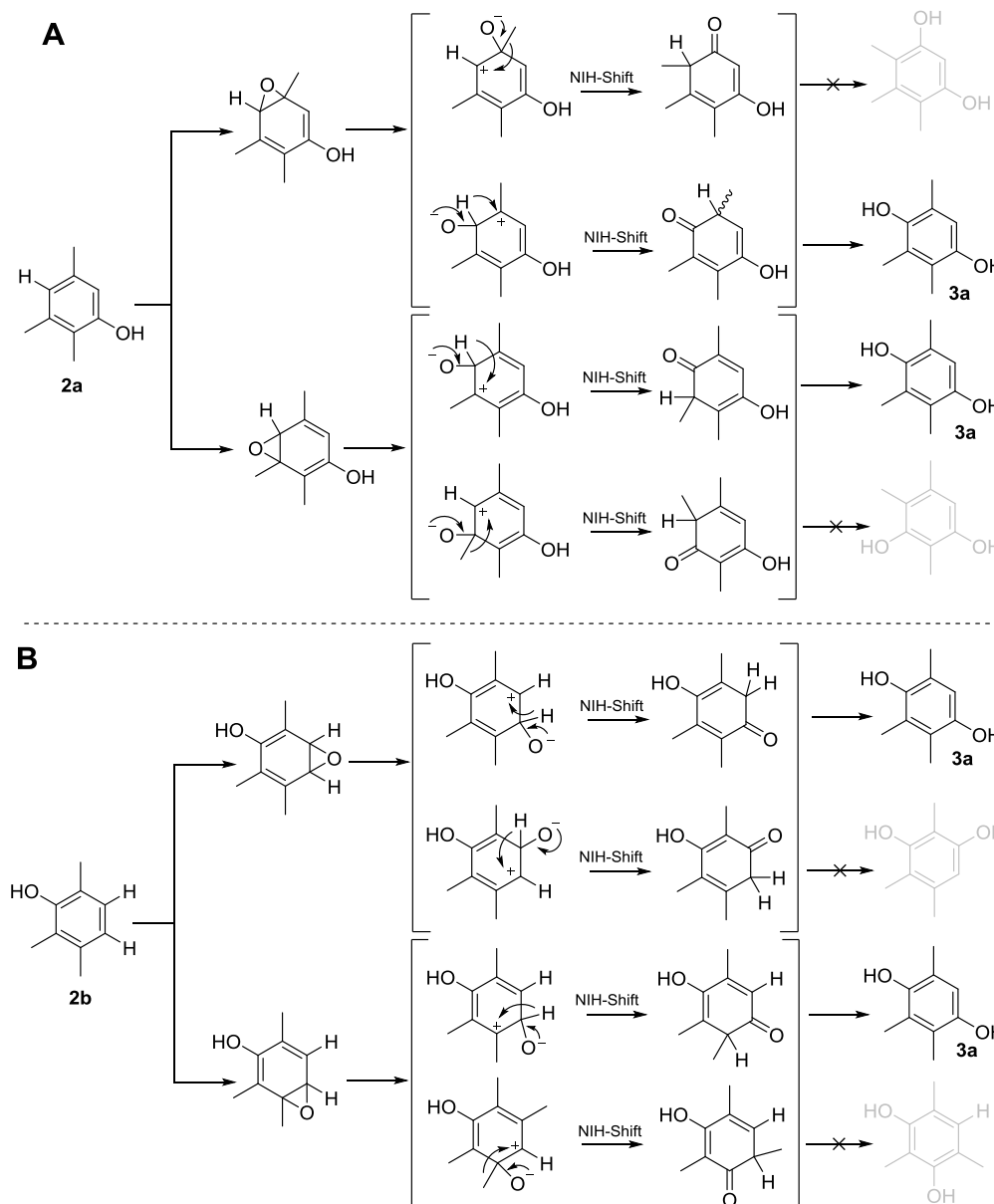
**Scheme 2.** Deduced substrate orientations and hydroxylation sites for conversion of **1a** with purified P450 BM3 (200  $\mu$ M NADPH supplemented). **A:** **1a** oriented with aryl carbon 4 toward compound I, leading preferentially to formation of **2b** and **2c**. **B:** **1a** oriented with benzylic carbons 1 and 2 toward compound I. Hydride abstraction leads to formation of an  $\alpha$ -carbon radical which after oxygen rebound yields **2e** and **2f** (major benzylalcohol products) during conversion of **1a**. Further information on benzene epoxidation, epoxide ring opening and re-aromatization can be found elsewhere.<sup>[12c, 17, 18b, 37]</sup>

Interestingly, the formation of **2d** (<2%) is not increased, indicating that aromatic hydroxylation is generally favored in absence of an *o*-CH<sub>3</sub>-substituent (Whitehouse et al.

could show that mutation F87A increases benzylic hydroxylation).<sup>[18b]</sup> The P450 BM3 WT produced less **2a** and **2b** (in total 13 to 17%) and only 3% of **3a** (Table 2). From this we assume that a different binding orientation of **1a** is predominant in the P450 BM3 WT active site as compared to P450 BM3 variant M3. This is in line with previous observations showing that binding orientations of the substrate are possibly more relevant for chemoselectivity than the intrinsic reactivity of the substrate.<sup>[12a, 18b]</sup> Scheme 2B shows the productive binding orientations for  $\alpha$ -benzylic hydroxylation of **1a**. Through formation of the  $\alpha$ -carbon radical at position 1 or 2 the predominant benzylalcohol products **2e** (40%) and **2f** (21%) are formed by P450 BM3 WT (Table 2, Entry 1). In case of P450 variant M3, the formation of **2e/2f** is decreased (29 and 9%) indicating again a different binding orientation of **1a** in the active site of BM3 WT as compared to P450 BM3 variant M2 and M3, which is supported by results from docking experiments. Further reasons for the change in chemo-selectivity during **1a** conversions could be: a) movements of the flexible protein backbone and in particular residue F87 during substrate binding and heme reduction<sup>[39]</sup> b) restricted space/ $\pi$ - $\pi$  interaction through introduction of A330F and c) binding of more than one substrate (steric crowding)<sup>[18b, 40]</sup>, which possibly acts as a decoy.<sup>[12c]</sup> The ability of decoys molecules to influence selectivity of P450 BM3 has been reported before.<sup>[12c, 41]</sup> Since the active site of P450 BM3 is large enough to bind bulky substrates such as naphthalene or steroids<sup>[33a, 42]</sup>, a second arene molecule could fit into the active site thus acting as potential decoy. This would lead to additional  $\pi$ - $\pi$  interactions in the active site that potentially influence substrate orientation and chemoselectivity. To solve these unanswered questions, a crystal structure of P450 BM3 WT and M3 with **1a** as ligand would be invaluable.

Di-hydroxylation of **1a/1b** or mono-hydroxylation of **2a/2b** and **2h** yielded mainly 1,4-dihydroxy compounds indicating a strong *p*-directing effect of phenolic-substituents (Scheme

3).<sup>[15, 30]</sup> Formation of trimethylresorcinol would be feasible, however requiring a methyl-group shift<sup>[18b]</sup>, which was not observed in this study.

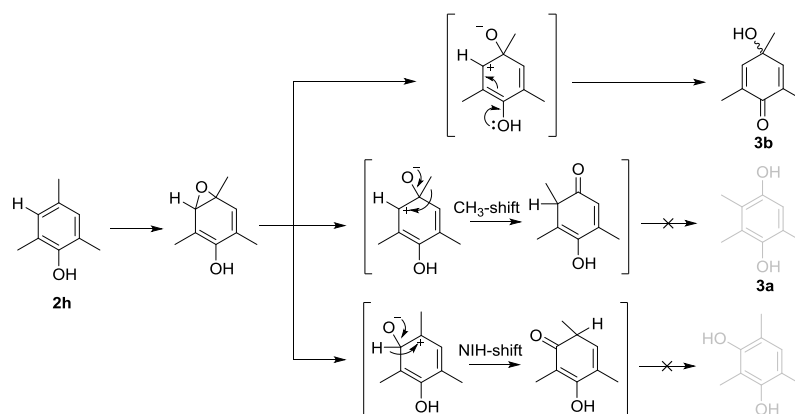


**Scheme 3.** Proposed routes to formation of TMHQ (**3a**) from **2a** (A) or **2b** (B). Resorcinol was not formed to a detectable amount therefore these pathways have to be excluded at the moment.

Di-hydroxylation of **1b** yielded a single product that was identified as *p*-quinol **3b**. For this, we propose a route that starts via 3,4-epoxidation of **2b** followed by epoxide ring opening and

finally affording the resonance stabilized *p*-quinol (Scheme 4), which cannot re-aromatize and therefore remains stable in solution.

Trimethylresorcinol or **3a** were not formed to a detectable amount and would require in both cases a methyl-group shift which is (in theory) feasible due to the lower BDE (bond dissociation energy) of C-C bonds compared to C-H bonds.



**Scheme 4.** Proposed route to formation of 4-hydroxy-2,4,6-trimethylcyclohexa-2,5-dien-1-one (**3b**) during conversion of **1b/2h**.

## Conclusions

Alternative enzymatic routes for vitamin E synthesis are important to match increasing demands. Here, we show the first direct aromatic hydroxylation of pseudocumene (**1a**) and mesitylene (**1b**) in water, with  $\text{O}_2$  and under mild reaction conditions to access five key phenolic  $\alpha$ -tocopherol synthons including a direct route to TMHQ (**3a**) and the first biocatalytic synthesis of the *p*-quinol **3b**. The P450 BM3 WT enzyme displayed highest selectivity for aromatic hydroxylation of **1b** (94%), whereas **1a** was hydroxylated at all six potential positions. A novel P450 BM3 variant (R47S, Y51W, I401M, A330F) had a boosted activity (23-fold) and improved coupling efficiency (3-fold) resulting in a 70-fold higher TOF for conversion of **1a**. For **1b** even a 230-fold improved TOF compared to P450 BM3WT

could be measured. Interestingly, conversions of **1a** with the engineered P450 BM3 variants M2 and M3 displayed altered chemoselectivity compared to P450 BM3 WT with increased formation of phenols as well as additional secondary hydroxylations. The unexpected over-oxidations yielded **3a** directly from **1a** (or **3b** from **1b**), which is a significant step toward more sustainable synthesis of vitamin E as the reaction can be performed in one-pot without the need for intermediate purification or additional catalysts. A product formation of 0.12 g L<sup>-1</sup> for **3a** (**1a** as substrate) is already a good starting point for further reaction and process engineering. Despite that a TTN of 5268 for **1a** is a good value for conversion of a non-natural substrate, additional enzyme engineering is necessary to improve operational performance and chemo-selectivity. Based on docking results and catalytic characterization we conclude that the mutation A330F provides new aromatic interactions ( $\pi$ -X- $\pi$ ) that improve binding and conversion of alkyl-benzenes. In agreement with previously published data on xylene hydroxylation, we observed that chemo-selectivity might not only be guided by the binding orientation, but also the substrate structure plays a key role. A constant pattern is visible in which the *o*-alkyl substituents (besides steric effects) promote  $\alpha$ -benzylic hydroxylations whereas aromatic hydroxylation is pre-dominant (>90%) when no *o*-substituent is present. It still remains unclear how P450 BM3 “decides” to catalyze aromatic or benzylic hydroxylation. The potentially intrinsic influence of methyl groups e.g. via carbon radical stabilization or altered BDE therefore seems to play an underestimated role during catalysis that requires deeper investigations. Based on the well-accepted enzymatic epoxidation mechanism of benzenes, epoxide ring opening (**3a** and **3b**) is strongly directed by phenolic substituents to obtain 1,4-hydroquinones with high selectivity. In summary, the obtained performance of P450 BM3 variant M3 indicates that a biocatalytic route to vitamin E has potential to become of commercial interest.

## Experimental Section

### Chemicals and reagents

All chemicals were obtained from Sigma Aldrich (Steinheim, Germany), abcr (Karlsruhe, Germany) or AppliChem (Darmstadt, Germany). Oligonucleotides were obtained at HPLC purity from Eurofins MWG Operon (Ebersberg, Germany). Plasmid extraction was done using a commercial Kit (QUIAGEN QIAprep Spin Miniprep Kit, Hilden, Germany). Glucose dehydrogenase (GDH) from *Pseudomonas sp.* and catalase from bovine liver were obtained from Sigma Aldrich (Steinheim, Germany). Phusion DNA polymerase, *DpnI* and dNTPs were purchased from Fermentas (St.Leon-Rot, Germany).

### Preparation and expression of site-saturation mutagenesis library on position A330

The saturation mutagenesis library on position A330 was prepared using variant M2 (R47S, Y51W, I401M) as template.<sup>[2a]</sup> Oligonucleotides for mutagenesis were designed according to the manual of the QuikChange Site-Directed mutagenesis Kit manual with following sequences: 5'- CAACTGCTCCTNNKTTTTCCCTATATGC-3' (forward primer) and 5'- GCATATAGGGAAAAMNNAGGAGCAGTTG-3' (reverse primer). Amplification of DNA for site-directed mutagenesis was achieved using a two-step PCR protocol with a previously reported PCR master mix composition and thermo cycler program.<sup>[2a]</sup> Successful amplification by PCR was verified by separating products on 0.8% agarose gel. After *DpnI* digest of template DNA for 4 h at 37 °C, plasmids were transformed into chemically competent *E. coli* BL21 lacI<sup>q1</sup> cells.<sup>[43]</sup> Sequencing of plasmids was done at MWG Eurofins DNA (Ebersberg, Germany) followed by analysis using Clone Manager 9 Professional Edition software (Scientific & Educational Software, Cary, NC, USA). Preparation of microtiter plates (MTPs), P450 BM3 expression and lysate preparation for screening in MTP format was done as described elsewhere in detail.<sup>[44]</sup>

### Screening and selection of variants for improved conversion of **1a**

The SSM library was screened with **1a** as substrate to identify a P450 BM3 variant that preferentially hydroxylates at aryllic carbons (positions 3 and 6). For this two 96 well MTPs (180 clones; 99.9% theoretical coverage)<sup>[29]</sup> were screened, by measuring the NADPH oxidation rate and formation of phenolic products using the 4-AAP detection system.<sup>[28]</sup> Each of the 96 wells contained 50  $\mu$ L protein lysate, 10% (v/v) DMSO, 200 mM **1a** (2 M stock in DMSO) and 130  $\mu$ L potassium phosphate buffer (KPi; 50 mM; pH 7.5). MTPs were incubated for 5 min before supplementation of 50  $\mu$ L NADPH (1 mM stock). Oxidation of NADPH was measured at 340 nm in a Tecan Sunrise MTP reader (Tecan Group Ltd., Männedorf, Switzerland). After full depletion of NADPH in the first wells, the reaction was quenched by pipetting 25  $\mu$ L quenching buffer (4 M urea in 0.1 M NaOH) into all wells. The regioselective 4-AAP assay for phenol detection was performed as described elsewhere.<sup>[28]</sup> After 30 min incubation the absorbance was measured at 509 nm in a Tecan Sunrise MTP reader to determine relative quantities of **2a** and **2b** by comparing these to the productivity of the template used for site saturation mutagenesis (variant M2).

### Expression, purification and biochemical characterization of P450 BM3

Expression of P450 BM3 in shake flasks and purification of the monooxygenase was achieved as described elsewhere.<sup>[44-45]</sup> Cell-free lysates cell pellets were prepared according to a published protocol.<sup>[15]</sup> Shortly, frozen cell pellets were lysed with lysozyme followed by sonication, centrifugation and freezing of cell-free supernatant in liquid N<sub>2</sub>. Finally, remaining water was removed overnight (16-20 h) under vacuum in a freeze-dryer. Kinetic characterizations were done using purified P450 protein at concentrations of 0.3  $\mu$ M (WT) and 0.1  $\mu$ M (P450 BM3 variant M2 and M3) which was determined by CO-binding assay following the protocol by Omura and Sato.<sup>[46]</sup> NADPH oxidation activity and coupling efficiency of the P450 variants and WT was measured as initial NADPH oxidation rates at

340 nm in 5 mL quartz glass cuvettes. For this, the reaction contained 10 mM of substrate (**1a/1b**; pre-solubilized in DMSO), 1.5% DMSO (V/V) in potassium phosphate buffer (KP; 50 mM; pH 7.5) in a final volume of 5 mL. After 5 min incubation, 200  $\mu$ M NADPH were supplemented and the oxidation of the cofactor was measured at 340 nm in a Varian Cary 50 UV spectrophotometer (Agilent Technologies, Darmstadt, Germany). After full depletion of NADPH, products were extracted twice with 500  $\mu$ L MTBE containing 1.5 mM 2,5-dimethylphenol (2,5-DMP) as internal standard. Organic phases were dried over anhydrous  $\text{MgSO}_4$  and combined for product analysis by GC-FID/-MS. Calibration curves for **2a-h** were prepared accordingly from analytical standards.

### **Conversion of 1a and 1b in presence of a cofactor regeneration system**

Regioselectivity, product yields and total turnover number (TTN) were determined using a GDH regeneration system for efficient regeneration of the NADPH cofactor.<sup>[47]</sup> If not stated otherwise, conversions of **1a** contained: 1  $\mu$ M P450 BM3 variant, 3 U GDH, 60 mM glucose, 1400  $\text{U mL}^{-1}$  catalase, 10 mM substrate, 2% DMSO (V/V), 400  $\mu$ M NADPH, 10 mM ascorbic acid in 50 mM phosphate buffer (pH 7.5). For the conversion of **1b**, a 4 mL reaction mixture was assembled containing 0.3  $\mu$ M P450 BM3 WT or 0.1  $\mu$ M of variant M2 or M3, 1.5% DMSO (V/V), 10 mM substrate, 30 mM glucose, 200  $\mu$ M NADPH, 1200  $\text{U mL}^{-1}$  catalase and 12 U GDH.

### **GC-FID and GC-MS analysis**

If not stated otherwise, products were extracted twice after 24 h conversion with 500  $\mu$ L MTBE containing 2,5-DMP (internal standard) as described in the previous section. Extracted products were analysed by GC-FID and GC-MS. For GC-FID measurements, 1  $\mu$ L of the organic phase was injected into a GC-2010-Plus chromatograph (Shimadzu GmbH, Duisburg, Germany) connected to a flame-ionization detector (FID) employing  $\text{H}_2$  as carrier gas.

Extracted compounds from conversion of **1a** were separated on a Hydrodex- $\beta$ -TBDAC column (Macherey Nagel, Düren, Germany). A temperature gradient was applied starting from 120 °C for 8 min, 7 °C min<sup>-1</sup> up to 210 °C and a final hold for 2 min at 210 °C.

Conversions of **1b** were separated isothermally at 140 °C on a FS Supreme 5 capillary column (Macherey Nagel, Düren, Germany; Figure S4). For GC-MS analysis a Shimadzu GC-2010 gas chromatograph (Duisburg, Germany) was used connected to a Shimadzu GC-MS QP2010S mass detector (Duisburg, Germany). Products resulting from conversions of **1a** were separated using the following program: 100 °C for 1 min, 3 °C min<sup>-1</sup> up to 150 °C, 15 °C min<sup>-1</sup> up to 250 °C, hold for 3 min (Optima 17 ms column). Further GC-MS analysis (**1b** conversions) was performed also using an Agilent 7890A GC-system equipped with an Agilent 5975C mass-selective detector. Separation was achieved using an Agilent HP-5MS column (30 m x 320  $\mu$ m, 0.25  $\mu$ m film) and the following program: 100 °C/hold 0.5 min; 10 °C min<sup>-1</sup> to 300 °C; hold 0 min.

### **<sup>1</sup>H- and <sup>13</sup>C-NMR analysis**

NMR spectra of **1a** conversions were measured on a Bruker Avance I 400 MHz NMR spectrometer. NMR spectra of **1b** conversions were measured on a Bruker Avance III 300 MHz NMR spectrometer. Chemical shifts are reported relative to TMS ( $\delta$ = 0.00 ppm). Coupling constants *J* are given in Hz.

### **Molecular modeling of P450 BM3 variants and docking of substrates**

For visualization, substrate docking and modelling of protein structures the P450 BM3 WT crystal structure (PDB ID: 1BU7) was used. The crystal structure model is available under <http://www.rcsb.org/pdb/home/home.do> (accessed 2017-01-20). The structure models of P450 BM3 M1 (R47S, Y51W), M2 (R47S, Y51W, I401M) and M3 (R47S, Y51W, A330F, I401M) were based on the aforementioned crystal structure of P450 BM3 WT and generated

by using Yasara Structure version 11.6.16 software.<sup>[32]</sup> Mutation(s) were introduced using swap option. The crystal structure of P450 BM3 as well as structure of the variants were further rotamerized and energy minimized to correct the residues that have non-standard torsion angles. Docking of substrates was carried out using VINA docking plug-in (25 independent runs)<sup>[48]</sup> within Yasara according to the default docking parameters from the example directory. The simulation cell was set to be 5 Å from the heme iron of P450 BM3. Visualization of the most meaningful docking results were prepared using Yasara software package.

## ASSOCIATED CONTENT

### Supporting Information

The Supporting Information (SI) includes results of GC and NMR analysis.

### Corresponding Author

\*e-mail, [u.schwaneberg@biotec.rwth-aachen.de](mailto:u.schwaneberg@biotec.rwth-aachen.de)

\*e-mail, [alexander.dennig@tugraz.at](mailto:alexander.dennig@tugraz.at)

\*e-mail, [aj.ruff@biotec.rwth-aachen.de](mailto:aj.ruff@biotec.rwth-aachen.de)

### Author Contributions

The manuscript was written through contributions of all authors. All authors have given approval to the final version of the manuscript. ‡These authors contributed equally.

## ACKNOWLEDGMENTS

We would like to acknowledge the EU funded 7th Framework project OXYGREEN (FP7-KBBE; Project Reference: 212281) for mesitylene related work. The work concerning pseudocumene has received funding from the European Union (EU) project ROBOX (Grant Agreement Nr. 635734) under EU's Horizon 2020 Programme Research and Innovation

actions H2020-LEIT BIO-2014-1. The authors thank Dr. Iwona Kaluzna and Dr. Monika Müller (both DSM, The Netherlands) for fruitful discussions and Ines Bachmann-Remy and Prof. Dr. Walter Leitner (Institute of Technical and Macromolecular Chemistry, RWTH Aachen) for NMR analysis. Furthermore we thank Marco Grull (RWTH Aachen) for experimental assistance.

## ABBREVIATIONS

TMP, trimethylphenol; NADP(H), nicotinamide adenine dinucleotide phosphate; TOF, turnover frequency; WT, wild type; TTN, total turnover number; CFE, cell free extracts; DMBA, dimethylbenzylalcohol; TMHQ, trimethylhydroquinone; MTP, microtiter plate.

## REFERENCES

- [1] H. Gröger, *Angew. Chem., Int. Ed. Engl.* **2014**, *53*, 3067-3069.
- [2] a) A. Dennig, J. Marienhagen, A. J. Ruff, L. Guddat, U. Schwaneberg, *ChemCatChem* **2012**, *4*, 771-773; b) R. J. Schmidt, *Appl. Catal., A* **2004**, *280*, 89-103.
- [3] a) E. Busto, R. C. Simon, W. Kroutil, *Angew. Chem., Int. Ed. Engl.* **2015**, *54*, 10899-10902; b) T. Netscher, *Vitam. Horm.* **2007**, *76*, 155-202; c) T. Netscher, *Angew. Chem., Int. Ed. Engl.* **2014**; d) R. C. Simon, E. Busto, N. Richter, V. Resch, K. N. Houk, W. Kroutil, *Nat. Commun.* **2016**, *7*, 13323.
- [4] T. Oku, Y. Arita, T. Ikariya, *Adv. Synth. Catal.* **2005**, *347*, 1553-1557.
- [5] H. Fiege, *Ullmann's Encyclopedia of Industrial Chemistry* **2000**.
- [6] a) R. Kannappan, S. C. Gupta, J. H. Kim, B. B. Aggarwal, *Genes Nutr.* **2012**, *7*, 43-52; b) A. C. Lindhorst, J. Schütz, T. Netscher, W. Bonrath, F. E. Kühn, *Catal. Sci. Technol.* **2017**; c) M. Uyanik, H. Hayashi, K. Ishihara, *Science* **2014**, *345*, 291-294.
- [7] A. A. Agaev, K. M. Madatzade, *Russ. J. Appl. Chem.* **2004**, *78*, 683-684.
- [8] a) R. D. Chambers, P. Goggin, W. K. R. Musgrave, *J. Chem. Soc.* **1959**, 1804-1807; b) O. A. Kholdeeva, I. V. Kozhevnikov, V. N. Sidel'nikov, V. A. Utkin, *Bull. Acad. Sci. USSR, Div. Chem. Sci.* **1989**, *38*, 1903-1907.
- [9] M. Tavanti, F. Parmeggiani, J. R. G. Castellanos, A. Mattevi, N. J. Turner, *ChemCatChem* **2017**.
- [10] W. Adam, W. A. Herrmann, J. Lin, C. R. Saha-Möller, R. W. Fischer, J. D. G. Correia, *Angew. Chem., Int. Ed. Engl.* **1994**, *106*, 2545-2546.
- [11] G. A. Olah, T. D. Ernst, *J. Org. Chem.* **1989**, *54*, 1204-1206.
- [12] a) A. Dennig, N. Lültsdorf, H. Liu, U. Schwaneberg, *Angew. Chem., Int. Ed. Engl.* **2013**, *52*, 8459-8462; b) F. Hollmann, I. W. C. E. Arends, K. Buehler, A. Schallmeyer, B. Bühler, *Green Chem.* **2011**, *13*, 226-265; c) O. Shoji, T. Kunimatsu, N. Kawakami, Y. Watanabe, *Angew. Chem., Int. Ed. Engl.* **2013**, *52*, 6606-6610; d) C. J. Whitehouse, S. G. Bell, L. L. Wong, *Chem. - Eur. J.* **2008**, *14*, 10905-10908; e) C. J. Whitehouse, S. G. Bell, L. L. Wong, *Chem. Soc. Rev.* **2012**, *41*, 1218-1260.
- [13] A. Karich, M. Kluge, R. Ullrich, M. Hofrichter, *AMB Express* **2013**, *3*, 5.
- [14] H. E. Schoemaker, D. Mink, M. G. Wubbolts, *Science* **2003**, *299*, 1694-1697.
- [15] A. Dennig, E. Busto, W. Kroutil, K. Faber, *ACS Catalysis* **2015**, *5*, 7503-7506.
- [16] B. Meunier, S. P. de Visser, S. Shaik, *Chem. Rev.* **2004**, *104*, 3947-3980.
- [17] S. P. de Visser, S. Shaik, *J. Am. Chem. Soc.* **2003**, *125*, 7413-7424.
- [18] a) C. J. Whitehouse, S. G. Bell, W. Yang, J. A. Yorke, C. F. Blanford, A. J. Strong, E. J. Morse, M. Bartlam, Z. Rao, L. L. Wong, *ChemBioChem* **2009**, *10*, 1654-1656; b) C. J. Whitehouse, N. H. Rees, S. G. Bell, L. L. Wong, *Chem. - Eur. J.* **2011**, *17*, 6862-

- 6868; c) C. J. Whitehouse, W. Yang, J. A. Yorke, B. C. Rowlatt, A. J. Strong, C. F. Blanford, S. G. Bell, M. Bartlam, L. L. Wong, Z. Rao, *ChemBioChem* **2010**, *11*, 2549-2556.
- [19] B. Bühler, A. Schmid, B. Hauer, B. Witholt, *J. Biol. Chem.* **2000**, *275*, 10085-10092.
- [20] J. H. Lee, B. Kim, W. J. Jin, J. W. Kim, H. H. Kim, H. Ha, Z. H. Lee, *Biochem. Pharmacol.* **2014**, *91*, 51-60.
- [21] a) M. C. Carreno, M. Gonzalez-Lopez, A. Urbano, *Angew. Chem., Int. Ed. Engl.* **2006**, *45*, 2737-2741; b) R. Sunasee, D. L. Clive, *Chem Commun (Camb)* **2010**, *46*, 701-703.
- [22] a) P. J. Loida, S. G. Sligar, *Biochemistry* **1993**, *32*, 11530-11538; b) A. W. Munro, D. G. Leys, K. J. McLean, K. R. Marshall, T. W. Ost, S. Daff, C. S. Miles, S. K. Chapman, D. A. Lysek, C. C. Moser, C. C. Page, P. L. Dutton, *Trends Biochem. Sci.* **2002**, *27*, 250-257.
- [23] C. A. Müller, B. Akkapurathu, T. Winkler, S. Staudt, W. Hummel, H. Gröger, U. Schwaneberg, *Adv. Synth. Catal.* **2013**, *355*, 1787-1798.
- [24] M. Bordeaux, A. Galarneau, J. Drone, *Angew. Chem., Int. Ed. Engl.* **2012**, *51*, 10712-10723.
- [25] A. Vidal-Limon, S. Aguila, M. Ayala, C. V. Batista, R. Vazquez-Duhalt, *J. Inorg. Biochem.* **2013**, *122*, 18-26.
- [26] C. T. Chiou, P. E. Porter, D. W. Schmedding, *Environ. Sci. Technol.* **1983**, *17*, 227-231.
- [27] C. McAuliffe, *J. Phys. Chem.* **1966**, *70*, 1267-1275.
- [28] T. S. Wong, N. Wu, D. Roccatano, M. Zacharias, U. Schwaneberg, *J. Biomol. Screening* **2005**, *10*, 246-252.
- [29] A. E. Firth, W. M. Patrick, *Nucleic Acids Res.* **2008**, *36*, W281-285.
- [30] W. T. Sulistyaningdyah, J. Ogawa, Q. S. Li, C. Maeda, Y. Yano, R. D. Schmid, S. Shimizu, *Appl. Microbiol. Biotechnol.* **2005**, *67*, 556-562.
- [31] V. A. Bushmelev, T. A. Kondrat'eva, M. A. Lipkin, A. V. Kondrat'ev, *Pharm. Chem. J.* **1992**, *25*, 340-349.
- [32] E. Krieger, G. Koraimann, G. Vriend, *Proteins* **2002**, *47*, 393-402.
- [33] a) S. Kille, F. E. Zilly, J. P. Acevedo, M. T. Reetz, *Nat. Chem.* **2011**, *3*, 738-743; b) O. Trott, A. J. Olson, *J. Comput. Chem.* **2010**, *31*, 455-461.
- [34] I. F. Sevrioukova, H. Li, H. Zhang, J. A. Peterson, T. L. Poulos, *Proc. Natl. Acad. Sci. U. S. A.* **1999**, *96*, 1863-1868.
- [35] L. M. Salonen, M. Ellermann, F. Diederich, *Angew. Chem., Int. Ed. Engl.* **2011**, *50*, 4808-4842.
- [36] L. A. Hammad, P. G. Wenthold, *J. Am. Chem. Soc.* **2001**, *123*, 12311-12317.
- [37] S. D. Munday, S. Dezvarei, I. C.-K. Lau, S. G. Bell, *ChemCatChem* **2017**.
- [38] G. da Silva, E. E. Moore, J. W. Bozzelli, *J. Phys. Chem. A* **2009**, *113*, 10264-10278.
- [39] S. Modi, M. J. Sutcliffe, W. U. Primrose, L. Y. Lian, G. C. Roberts, *Nat. Struct. Biol.* **1996**, *3*, 414-417.
- [40] J. P. Harrelson, W. M. Atkins, S. D. Nelson, *Biochemistry* **2008**, *47*, 2978-2988.
- [41] F. E. Zilly, J. P. Acevedo, W. Augustyniak, A. Deege, U. W. Hausig, M. T. Reetz, *Angew. Chem., Int. Ed. Engl.* **2011**, *50*, 2720-2724.
- [42] D. Appel, S. Lutz-Wahl, P. Fischer, U. Schwaneberg, R. D. Schmid, *J. Biotechnol.* **2001**, *88*, 167-171.
- [43] M. Blanusa, A. Schenk, H. Sadeghi, J. Marienhagen, U. Schwaneberg, *Anal. Biochem.* **2010**, *406*, 141-146.
- [44] J. Nazor, S. Dannenmann, R. O. Adjei, Y. B. Fordjour, I. T. Ghampson, M. Blanusa, D. Roccatano, U. Schwaneberg, *Protein Eng. Des. Sel.* **2008**, *21*, 29-35.
- [45] U. Schwaneberg, A. Sprauer, C. Schmidt-Dannert, R. D. Schmid, *J. Chromatogr. A* **1999**, *848*, 149-159.

- [46] a) T. Omura, R. Sato, *J. Biol. Chem.* **1964**, 239, 2379-2385; b) T. Omura, R. Sato, *J. Biol. Chem.* **1964**, 239, 2370-2378.
- [47] C. A. Müller, B. Akkapurathu, T. Winkler, S. Staudt, W. Hummerl, H. Gröger, U. Schwaneberg, *Adv. Synth. & Catalysis* **2013**, 355, 1787-1798.
- [48] O. Trott, A. J. Olson, *Computational Chemistry* **2009**, 31, 455-461.

## TOC Graphical Abstract

